

FrsA functions as a cofactor-independent decarboxylase to control metabolic flux

Kyung-Jo Lee^{1,7}, Chang-Sook Jeong^{2,7}, Young Jun An², Hyun-Jung Lee¹, Soon-Jung Park³, Yeong-Jae Seok⁴, Pil Kim⁵, Jung-Hyun Lee^{2,6}, Kyu-Ho Lee^{1*} & Sun-Shin Cha^{2,6*}

The interaction between fermentation-respiration switch (FrsA) protein and glucose-specific enzyme IIA^{Glc} increases glucose fermentation under oxygen-limited conditions. We show that FrsA converts pyruvate to acetaldehyde and carbon dioxide in a cofactor-independent manner and that its pyruvate decarboxylation activity is enhanced by the dephosphorylated form of IIA^{Glc} (d-IIA^{Glc}). Crystal structures of FrsA and its complex with d-IIA^{Glc} revealed residues required for catalysis as well as the structural basis for the activation by d-IIA^{Glc}.

The bacterial phosphoenolpyruvate:sugar phosphotransferase system (PTS) mediates a series of phosphorylation and dephosphorylation reactions coupled to translocation of certain sugars across the cytoplasmic membrane. Glucose transport involves the four components of PTS: enzyme I, histidine phosphocarrier protein, glucose-specific enzyme IIA^{Glc} and the membrane-bound enzyme IICB^{Glc}. When glucose is imported, phosphoryl transfer occurs sequentially from phosphoenolpyruvate to enzyme I, histidine phosphocarrier protein, IIA^{Glc}, IICB^{Glc} and finally glucose. In addition, the PTS components regulate a variety of physiological processes through direct interactions with their target proteins^{1–5}. For example, d-IIA^{Glc} inhibits transport of non-PTS sugars by interacting with their transporters¹, and the phosphorylated form of IIA^{Glc} (p-IIA^{Glc}) activates cyclic AMP synthesis by interacting with adenylate cyclases².

FrsA, which was initially isolated from a pool of d-IIA^{Glc}-binding proteins, acts as a fermentation-respiration switch involved in the metabolic transition to increased fermentation of glucose in *Escherichia coli*⁶. Disruption of the *frsA* gene increases the respiration rate of *E. coli* in the presence of glucose as a carbon source, whereas high FrsA expression promotes fermentation-oriented metabolisms with the concomitant accumulation of mixed-acid fermentation products even under aerobic conditions. Despite the physiological implication of FrsA in metabolism, its function remains unknown at the biochemical level. FrsA is predicted to have an α/β -hydrolase fold domain, but it shows no hydrolase activity⁶.

As pyruvate catabolism is the branching point between respiration and fermentation in the metabolic pathway of glucose, we first examined whether FrsA could use pyruvate as a substrate. We selected *Vibrio vulnificus* FrsA for this study because its recombinant form is more highly expressed in the *E. coli* overexpression system than those of other orthologs of FrsA, which can be found in a range of facultative anaerobes⁶. Addition of the purified FrsA (Supplementary Fig. 1) to a reaction mixture containing pyruvate resulted in a decrease of pyruvate concentration in an FrsA concentration-dependent manner (Fig. 1a). Analysis of ¹H NMR spectra revealed that the decrease in

pyruvate concentration was accompanied by the production of acetaldehyde (Supplementary Results, Supplementary Fig. 2), indicating that FrsA converted pyruvate into acetaldehyde and a one-carbon compound that we presumed to be carbon dioxide. Direct estimation of reaction mixtures containing various concentrations of pyruvate in the presence of the purified FrsA verified the production of both acetaldehyde and carbon dioxide with a 1:1 ratio (Fig. 1b). To exclude the possibility that this reaction had been catalyzed by minute quantities of contaminants that might exist in the purified FrsA prepared from *E. coli*, we added crude lysates of wild-type or the *frsA* deletion mutant strains of *E. coli*⁶ to a solution containing pyruvate. We saw no production of acetaldehyde in the solution with the *frsA*-deletion mutant lysate, whereas we did observe acetaldehyde production in the solution with the wild-type lysate, in a lysate concentration-dependent manner (Supplementary Fig. 3), indicating that FrsA itself performed the breakdown of pyruvate. Substrate-specificity analyses indicated that other carboxylate-containing metabolites were not used by FrsA (Supplementary Fig. 4).

To examine whether FrsA uses pyruvate as a substrate *in vivo*, we measured the cellular concentrations of pyruvate and acetaldehyde in wild-type and *frsA* deletion mutant *V. vulnificus* strains grown in the presence of glucose. The cellular concentration of pyruvate in the *frsA* deletion mutant was increased by approximately three-fold and the acetaldehyde concentration reduced by 40% as compared to the wild-type strain under anaerobic culture conditions, whereas the mutant and wild-type strains showed similar pyruvate concentrations under aerobic culture conditions (Fig. 1c). The accumulation of pyruvate in the mutant strain grown under anaerobic conditions indicated that the *frsA* disruption caused a defect in pyruvate consumption via the fermentative metabolic pathway. The cellular concentrations of pyruvate and acetaldehyde returned to wild-type levels when we introduced the intact *frsA* gene into the mutant strain (Fig. 1c). The lack of an apparent effect of FrsA on the bacterial cells grown under aerobic conditions might result from reduced expression of FrsA in the presence of oxygen via unknown regulatory mechanisms. These results indicated that FrsA is involved in pyruvate catabolism *in vivo*. Consequently, we concluded that FrsA catalyzes nonoxidative pyruvate decarboxylation, which fits its physiological function of promoting fermentation. According to steady-state kinetics, FrsA is a proficient enzyme with k_{cat} and k_{cat}/K_m values of 1,372 s⁻¹ and 3,518 s⁻¹ mM⁻¹, respectively (Table 1 and Supplementary Fig. 5).

To our knowledge, FrsA is the first decarboxylase found to have the α/β -hydrolase fold. To elucidate why FrsA shows no hydrolytic

¹Department of Environmental Science, Hankuk University of Foreign Studies, Yongin, Republic of Korea. ²Marine Biotechnology Research Center, Korea Ocean Research & Development Institute (KORDI), Ansan, Republic of Korea. ³Department of Environmental Medical Biology and Institute of Tropical Medicine, The Brain Korea 21 Project, Yonsei University College of Medicine, Seoul, Republic of Korea. ⁴Department of Biophysics and Chemical Biology, Seoul National University, Seoul, Republic of Korea. ⁵Department of Biotechnology, The Catholic University of Korea, Bucheon, Republic of Korea. ⁶Department of Marine Biotechnology, University of Science and Technology, Daejeon, Republic of Korea. ⁷These authors contributed equally to this work. *e-mail: khlee@hufs.ac.kr or chajung@kordi.re.kr

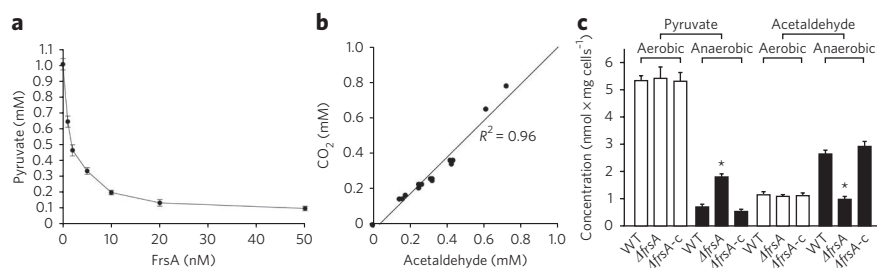


Figure 1 | Enzymatic activity of FrsA. (a) Decomposition of pyruvate by the recombinant FrsA. Pyruvate (1 mM) was added to reactions with varying FrsA. Pyruvate remaining after 5 min incubation was measured and is presented as the averages and s.d. from three independent assays. (b) Production of acetaldehyde and CO₂ in the FrsA-catalyzed reaction. Concentrations of acetaldehyde and CO₂ were measured in reactions containing 1 nM FrsA and varying pyruvate. Produced acetaldehyde and CO₂ in each mixture were plotted and subjected to a linear regression analysis. (c) Cellular concentrations of pyruvate and acetaldehyde in the wild-type strain carrying a broad-host-range vector pRK415 (WT), the Δ frsA mutant carrying pRK415 (Δ frsA) and the Δ frsA mutant carrying pRK415-frsA (Δ frsA-c). Bacterial cells grown in LBS-glucose medium under aerobic or anaerobic conditions were treated as previously described²³. The levels of pyruvate and acetaldehyde are presented with the averages and s.d. from three independent assays. An asterisk indicates $P < 0.0001$ (Student's *t* test).

activity and how pyruvate decarboxylation occurs in the context of the α/β -hydrolase structure, we determined the crystal structure of FrsA (Fig. 2a). FrsA yielded monoclinic crystals with two FrsA molecules (FrsA-I and FrsA-II) in an asymmetric unit. The interactions between FrsA molecules within crystals were not extensive, indicating that FrsA is a monomeric protein. Consistently, FrsA was eluted as a monomer in gel filtration experiments (Supplementary Fig. 6). The structures of FrsA-I and FrsA-II are virtually identical except for the putative active site conformation (Supplementary Fig. 7). FrsA is a two-domain protein with an N-terminal helical domain (residues 1–165) and a C-terminal domain adopting the canonical α/β -hydrolase fold (residues 166–415), and a cavity exists at the domain interface (Fig. 2a). The nucleophile elbow is the most conserved strand-turn-helix motif (β 5-turn- α 13 in FrsA) among α/β -hydrolases (Fig. 2a). In this motif, a nucleophilic residue such as a cysteine, serine or aspartate residue takes a position in the turn region of the motif, forming a catalytic triad, a hydrolytic device, with a histidine and an aspartate (or glutamate) in the vicinity^{7,8}. In FrsA, however, Arg272 exists at the nucleophile elbow and there is no nearby histidine, which is the structural basis for the lack of hydrolytic activity of FrsA despite its α/β -hydrolase structure.

Simple α -keto acids such as pyruvate lack an electron sink to accommodate the negative charge developed upon decarboxylation. Therefore, most decarboxylating enzymes are associated with cofactors facilitating decarboxylation to stabilize a carbanion generated upon the cleavage of the carbon-carbon bond linking the carboxylate group to its adjacent carbon. However, there is no coenzyme or metal in the active site of FrsA. So far, a cofactor-independent decarboxylation mechanism has been described in two enzymes: orotidine 5'-monophosphate (OMP) decarboxylase^{9–13} and 2-oxo-4-hydroxy-4-carboxy-5-ureidoimidazole decarboxylase^{14,15}. Direct decarboxylation in both enzymes is based on electrostatic repulsion between two closely located carboxylate groups, one in the enzyme and one in the substrate. The ground-state destabilization caused by the electrostatic repulsion is believed to facilitate decarboxylation^{9–15}. As our efforts to prepare a crystal of the FrsA-pyruvate complex were not successful, we instead created a model for the FrsA-pyruvate complex to get insights into the reaction mechanism, presuming that the cavity at the domain interface is the active site (see Supplementary Methods and Fig. 2b). The inside of this site is mainly lined by hydrophobic residues (Leu202, Phe273, Phe303, Tyr316, Leu320, Met338 and Trp341), which could interact with the methyl group of

pyruvate, and an oxyanion hole could interact with the carbonyl oxygen. Three charged residues (Arg53, Asp203 and Arg272) are clustered against the hydrophobic background (Fig. 2b and Supplementary Fig. 8). In analogy to the role of electrostatic repulsion in currently known cofactor-independent decarboxylations, we noted that Asp203 is located at the bottom of the active site and conserved in all FrsA orthologs (Supplementary Fig. 9). An alanine or an isosteric asparagine substitution of this residue completely abolished the enzymatic activity (Table 1), demonstrating the critical role of the carboxylate group of Asp203 in catalysis. According to the enzymatic mechanism of OMP decarboxylase, the ammonium group of a nearby lysine residue donates a proton to the carbanion originated from decarboxylation^{9–12}. On the basis of this knowledge, we examined the catalytic contribution of the two arginine residues. Single point mutations resulting in alanine substitution (R53A or R272A) led to relatively minor alterations of enzymatic activity, but alanine substitution of both basic

residues led to the complete loss of the enzymatic activity (Table 1), revealing that both residues contribute to catalysis.

FrsA has a bell-shaped profile of k_{cat} and k_{cat}/K_m versus pH, with a maximum at pH = ~7 (Supplementary Fig. 10), as OMP decarboxylase does¹⁰. An optimal enzymatic activity at neutral pH suggests that deprotonated Asp203 and protonated Arg53 and Arg272 are required for FrsA's catalytic activity, supporting a direct decarboxylation mechanism based on electrostatic repulsion. In the case of OMP decarboxylase, nonreactive parts of substrates interact extensively with enzymes to provide the binding energy needed to closely locate two carboxylate groups, in a process that has been called the Circe effect¹⁶. Likewise, the nonreactive parts of pyruvate (a methyl group and a carbonyl group) would form favorable contacts with FrsA, compensating for the electrostatic repulsion between two carboxylate groups in proximity. Although our complex model gave a clue to the mode of interaction between FrsA and pyruvate (Fig. 2b and Supplementary Fig. 8), a detailed analysis of these interactions awaits future study.

Nonoxidative pyruvate decarboxylation is a key reaction in the mixed-acid fermentation of glucose, and IIA^{Glc} is dephosphorylated in the presence of glucose. To understand how the glucose-dependent switch in IIA^{Glc} phosphorylation state might affect FrsA function, we investigated the mechanisms and consequences of FrsA forming a tight complex with d-IIA^{Glc} *in vivo* and *in vitro*⁶. We measured the kinetic parameters of FrsA in the presence of IIA^{Glc}. Remarkably, the enzyme

Table 1 | Kinetic parameters for FrsA^a and other PDCs

Protein ^b	K_m (mM)	k_{cat} (sec ⁻¹)	k_{cat}/K_m (sec ⁻¹ mM ⁻¹)
WT	0.39 ± 0.02	1,372 ± 11	3,518 ± 183
R53A	0.52 ± 0.04	845 ± 42	1,625 ± 149
D203A ^c	∞	NA	NA
D203N ^c	∞	NA	NA
R272A	0.45 ± 0.03	589 ± 26	1,309 ± 104
R53A/R272A ^c	∞	NA	NA
WT + dephospho-IIA ^{Glc}	0.39 ± 0.03	2,980 ± 158	7,641 ± 713
WT + phospho-IIA ^{Glc}	0.39 ± 0.01	1,311 ± 48	3,362 ± 150
<i>Z. mobilis</i> PDC ²⁴	0.4	180	450
<i>S. cerevisiae</i> PDC ²⁵	2.29	73	32

^aAverages and s.d. were derived from at least two independent assays. ^bFrsA unless otherwise specified. ^cParameters could not be measured as enzymes were not active.

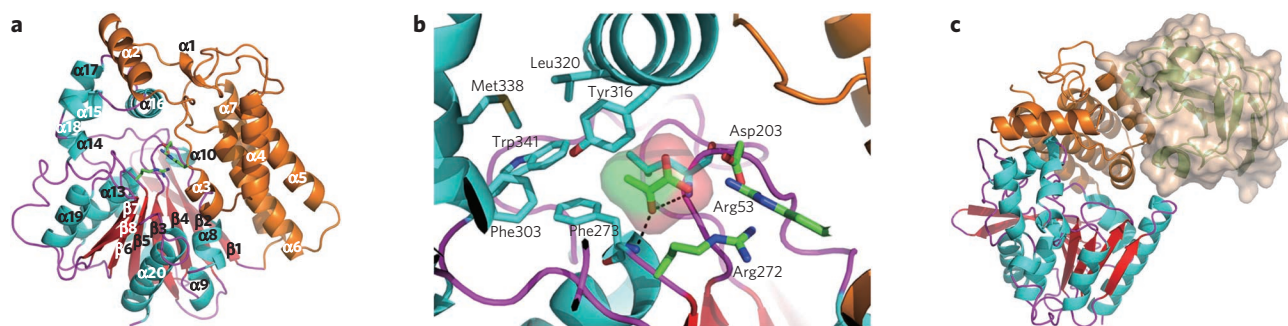


Figure 2 | Structures of FrsA and the FrsA-d-IIA^{Glc} complex. (a) Ribbon diagram of FrsA-I. The N-terminal helical domain is colored in orange. In the C-terminal α/β -domain, helices, strands and coils are colored in cyan, red and magenta, respectively. The catalytic residues (Arg53, Asp203 and Arg272) are in stick form. (b) Residues in proximity to pyruvate are shown in stick form and labeled. Pyruvate is veiled by a transparent surface. Black dashed lines represent plausible hydrogen bonds. (c) Ribbon diagram of the FrsA-d-IIA^{Glc} complex. d-IIA^{Glc} is veiled by a transparent surface.

activity of FrsA was enhanced by d-IIA^{Glc}, whereas it was not affected by p-IIA^{Glc} (Table 1). Therefore, the enhancement of the FrsA activity by d-IIA^{Glc} explains why FrsA promotes the fermentative metabolism of glucose. To learn more about how this change occurs, we determined the crystal structure of the FrsA-d-IIA^{Glc} complex (Fig. 2c and Supplementary Figs. 11 and 12). We observed that Glu68 of FrsA is located in the vicinity of the phosphorylation site (His90) of d-IIA^{Glc} (Supplementary Fig. 13), suggesting that a negative repulsion between these two groups might destabilize a complex between FrsA and p-IIA^{Glc}. Additionally, FrsA in the d-IIA^{Glc} complex structure more closely resembled FrsA-I from the structure of FrsA alone, in which the active site was more accessible; in comparison, FrsA-II contained an extended helix that overlapped with the active site (Supplementary Figs. 14 and 15). As a result, we concluded that d-IIA^{Glc} enhances the enzymatic activity of FrsA by stabilizing or promoting this 'open', active form.

Oxygen levels are considerably lower, and glucose levels are much higher, in mammalian tissues than in ambient environments^{17,18}. Because pathogens should rely mainly on fermentative metabolisms of glucose under this oxygen-limited circumstance, it would be advantageous to decarboxylate pyruvate generated from glucose without generating NADH. In addition, FrsA exists in a complex with d-IIA^{Glc} under these conditions, which would result in enhanced enzymatic activity. Thus, FrsA might be involved in the pathogenicity of facultative anaerobic pathogens. Disruption of the *frsA* gene in *V. vulnificus* reduced its virulence; the half-maximal infectious dose of the deletion mutant was ten times higher than that of its isogenic wild-type strain in mouse mortality tests (Supplementary Table 1).

The nonoxidative decarboxylation of pyruvate is catalyzed by pyruvate decarboxylase (PDC; EC 4.1.1.1) with thiamine pyrophosphate as a coenzyme^{19–21}. PDC is widespread in plants and yeast but is absent in animals and rare in prokaryotes²². There has been no protein predicted to have nonoxidative pyruvate decarboxylation activity in sequenced genomes of facultative anaerobic bacteria harboring FrsA, although such an enzymatic activity is required for their efficient glucose fermentation. Therefore, the pyruvate decarboxylation activity of FrsA, which is superior to that of yeast (*Saccharomyces cerevisiae*) or *Zymomonas mobilis* PDCs (Table 1), so far considered the most proficient PDCs, opens a new avenue toward understanding the physiology of facultative anaerobiosis.

Accession codes. The nucleotide sequence of *V. vulnificus frsA* has been submitted to GenBank Gene and the European Bioinformatics Institute Data Bank with accession number HM172799. The atomic coordinates of FrsA (code 3MVE) and the FrsA-d-IIA^{Glc} complex (code 3OUR) have been deposited in the Protein Data Bank.

Received 29 September 2010; accepted 7 April 2011; published online 29 May 2011

References

- Saier, M.H. Jr., Novotny, M.J., Comeau-Fuhrman, D., Osumi, T. & Desai, J.D. *J. Bacteriol.* **155**, 1351–1357 (1983).
- Peterkofsky, A. *et al. Prog. Nucleic Acid Res. Mol. Biol.* **44**, 31–65 (1993).
- Nam, T.W. *et al. Proc. Natl. Acad. Sci. USA* **105**, 3751–3756 (2008).
- Seok, Y.J. *et al. J. Biol. Chem.* **272**, 26511–26521 (1997).
- Kim, Y.J. *et al. FEBS Lett.* **584**, 4537–4544 (2010).
- Koo, B.M. *et al. J. Biol. Chem.* **279**, 31613–31621 (2004).
- Ollis, D.L. *et al. Protein Eng.* **5**, 197–211 (1992).
- Lee, S.J. *et al. J. Biol. Chem.* **278**, 44552–44559 (2003).
- Wu, N., Mo, Y., Gao, J. & Pai, E.F. *Proc. Natl. Acad. Sci. USA* **97**, 2017–2022 (2000).
- Appleby, T.C., Kinsland, C., Begley, T.P. & Ealick, S.E. *Proc. Natl. Acad. Sci. USA* **97**, 2005–2010 (2000).
- Harris, P., Navarro Poulsen, J.C., Jensen, K.F. & Larsen, S. *Biochemistry* **39**, 4217–4224 (2000).
- Miller, B.G., Hassell, A.M., Wolfenden, R., Milburn, M.V. & Short, S.A. *Proc. Natl. Acad. Sci. USA* **97**, 2011–2016 (2000).
- Chan, K.K. *et al. Biochemistry* **48**, 5518–5531 (2009).
- Cendron, L. *et al. J. Biol. Chem.* **282**, 18182–18189 (2007).
- Kim, K., Park, J. & Rhee, S. *J. Biol. Chem.* **282**, 23457–23464 (2007).
- Jencks, W.P. *Adv. Enzymol.* **43**, 219–410 (1975).
- Erecińska, M. & Silver, I.A. *Respir. Physiol.* **128**, 263–276 (2001).
- Chun, C.D., Liu, O.W. & Madhani, H.D. *PLoS Pathog.* **3**, e22 (2007).
- Arjunan, P. *et al. J. Mol. Biol.* **256**, 590–600 (1996).
- Dobritzsch, D., König, S., Schneider, G. & Lu, G. *J. Biol. Chem.* **273**, 20196–20204 (1998).
- Dyda, F. *et al. Biochemistry* **32**, 6165–6170 (1993).
- Stephenson, M.P. & Dawes, E.A. *J. Gen. Microbiol.* **69**, 331–343 (1971).
- Hogema, B.M. *et al. Mol. Microbiol.* **30**, 487–498 (1998).
- Bringer-Meyer, S., Schimz, K.L. & Sahm, H. *Arch. Microbiol.* **146**, 105–110 (1986).
- Sergienko, E.A. & Jordan, F. *Biochemistry* **40**, 7369–7381 (2001).

Acknowledgments

We are grateful to Y.-J. Lee, H.-S. Lee, S.J. Chung and J.K. Lee for comments on the manuscript. This work was supported by the Marine and Extreme Genome Research Center program of Ministry of Land, Transport and Maritime Affairs, the Mid-career Researcher Program through National Research Foundation grant funded by the Ministry of Education, Science and Technology (2009-0092822), a KORDI in-house program (PE98513) and the Development of Biohydrogen Production Technology Using Hyperthermophilic Archaea program of Ministry of Land, Transport and Maritime Affairs.

Author contributions

S.-S.C. and K.-H.L. designed the project, analyzed data and wrote the manuscript. K.-J.L., C.-S.J., Y.J.A., H.-J.L., S.-J.P. and S.-S.C. performed experiments. Y.-J.S. gave advice on the design of this project and the NMR experiments. P.K. gave advice on the biochemical experiments. J.-H.L. contributed analytic tools.

Competing financial interests

The authors declare no competing financial interests.

Additional information

Supplementary information is available online at <http://www.nature.com/naturechemicalbiology/>. Reprints and permissions information is available online at <http://www.nature.com/reprints/index.html>. Correspondence and requests for materials should be addressed to S.-S.C. or K.-H.L.